ASTROPARTICLE THEORY: SOME NEW INSIGHTS INTO HIGH ENERGY COSMIC RAYS

ESTEBAN ROULET
CONICET, Centro Atómico Bariloche, 8400, Argentina
E-mail: roulet@cab.cnea.gov.ar

Some new developments obtained in the last few years concerning the propagation of high energy cosmic rays are discussed. In particular, it is shown how the inclusion of drift effects in the transport diffusion equations leads naturally to an explanation for the knee, for the second knee and for the observed behavior of the composition and anisotropies between the knee and the ankle. It is shown that the trend towards a heavier composition above the knee has significant impact on the predicted neutrino fluxes above 10^{14} eV. The effects of magnetic lensing on the cosmic rays with energies above the ankle are also discussed, analyzing the main features of the different regimes that appear between the diffusive behavior that takes place at lower energies and the regime of small deflections present at the highest ones.

1 Introduction

Since their discovery in 1912, cosmic rays (CRs) were of great help for particle physics, providing a source of high energy particles for free, which only required the construction of detectors in order to observe different kinds of interesting phenomena. In this way, positrons, muons, pions, kaons and hyperons were discovered in the period 1930–1950. However, when after the '50s man made accelerators reached energies beyond the GeV, particle physics moved back to the labs and cosmic ray research became focused on the study of the CRs themselves (rather than on the products of their interactions), trying to understand their origin, the mechanisms responsible for their acceleration and the way they propagate from the sources up to us.

There are only a few observable quantities associated to the CR fluxes. These are the energy spectrum, the CR composition and the anisotropies in arrival directions, and it is through their study that the CR mysteries have to be unraveled. For instance, the fact that the spectrum is essentially a power law and not a thermal one is what led Fermi to suggest that the CR acceleration was a stochastic process. Also, looking at low energy cosmic rays, the study of the abundances of spallation products (like Li, Be and B, which are produced mainly by spallation of C, N and O) gives information about the amount of matter traversed by the CRs, while the abundances of unstable isotopes (e.g. ^{10}Be) gives information on the time spent by CRs in the Galaxy. On the other hand, the anisotropies observed on the low energy CRs arriving from the East and from the West gave indications that they were caused by the deflections produced by the geomagnetic field on the positively charged CRs.

Many puzzles are also associated with the observed properties of the CRs with very high energies, those above 10^{15} eV and up to the highest ones exceeding 10^{20} eV. In particular, we would like to know what causes the spectral changes observed, what is the origin of the observed anisotropies and the changes in composition as a function of energy and how CR sources would look like at ultrahigh energies. As will be discussed below, a crucial issue in this respect is to understand in detail the propagation of CRs through the magnetic fields present in the Galaxy, since this is essential to determine their properties when we finally observe them.

2 The cosmic ray spectrum

The differential flux of CRs changes by more than 30 orders of magnitude in the energy range from 10^9 eV to 10^{20} eV, following essentially a power law $E^{-\alpha}$ which shows only some small but noticeable breaks in the power index α. One has indeed $\alpha \simeq 2.6 \div 2.7$ at low energies, with a steepening to $\alpha \simeq 3$ at the so-called *knee*, which takes place at $E_k \simeq 3 \times 10^{15}$ eV. A second steepening to $\alpha \simeq 3.3$, referred to as the *second knee*, has been reported at $E_{sk} \simeq 4 \times 10^{17}$ eV, while a hardening to $\alpha \simeq 2.7$ takes place at $E_a \simeq 5 \times 10^{18}$ eV, being known as the *ankle*. These general features are apparent in the data[1] shown in Fig. 1, which displays the quantity $E^3 \times \mathrm{d}\Phi/\mathrm{d}E$. The observed spectrum is just a reflection of the original source spectra which have been

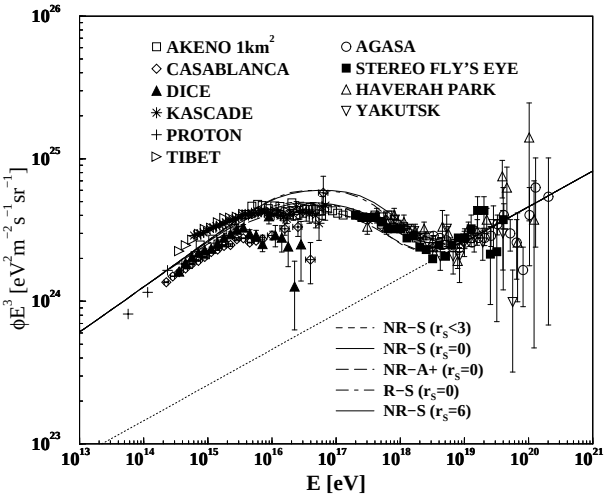

Figure 1. CR spectrum as measured by different experiments and predictions of the diffusion/drift scenario for different galactic models. The dotted line is the assumed extragalactic flux.

reshaped by the energy dependence of the confinement time of CRs in the Galaxy, since for increasing energies CRs escape more readily and hence their local density becomes less enhanced. To understand this last effect we will then discuss in some detail the transport of CRs through the magnetic fields permeating the Galaxy. Beyond the ankle the CRs are no longer confined inside the Galaxy (and most likely there are no galactic sources reaching such high energies) so that a transition to an extragalactic component should be taking place there.

2.1 Cosmic ray diffusion and drift:

Our Galaxy is believed to have a regular and a random magnetic field, both with local strength of a few μG. The regular component is aligned with the spiral arms, reversing its directions between consecutive arms and having a typical scale height of ~ 1 kpc. Also a more extended halo component is believed to exist, with typical scale height of a few kiloparsecs but its symmetry properties are less well established. On the other hand, the random component has a spectrum not very different from a Kolmogorov one (as would result if its origin is associated with the turbulence in the interstellar medium (ISM)), i.e. with a magnetic energy density satisfying $\mathrm{d}E_r/\mathrm{d}k \propto k^{-5/3}$ in Fourier space, with a maximum scale of turbulence of order $L_{max} \simeq 100$ pc.

When particles of charge Ze propagate across a regular field $\mathbf{B}_0$, they describe helical trajectories characterized by a pitch angle θ, so that the component of the velocity parallel to $\mathbf{B}_0$ is $v_\parallel = c\cos\theta$, and a Larmor radius given by

$$r_L = \frac{pc}{ZeB_0} \simeq \frac{E/Z}{10^{15}\ \mathrm{eV}}\frac{\mu\mathrm{G}}{B_0}\mathrm{pc} \qquad (1)$$

(the radius of the helical trajectory is $r_L \sin\theta$). In the presence of the random component $\mathbf{B}_r$, the CRs will scatter off the magnetic field irregularities with associated scales of order r_L, changing their pitch angle but not their velocity. This will lead to a random walk and a diffusion along the magnetic field direction characterized by a diffusion coefficient

$$D_\parallel = \frac{\langle \Delta x_\parallel^2 \rangle}{2\Delta t} = \frac{c}{3}\lambda_\parallel, \qquad (2)$$

where $\lambda_\parallel$ is the pitch angle scattering length, which depends on how much power there is in the magnetic field modes at scales $\sim r_L$, i.e.

$$\lambda_\parallel \propto \left.\frac{r_L}{\mathrm{d}E_r/\mathrm{d}\ \ln k}\right|_{k=2\pi/r_L}. \qquad (3)$$

Hence, for a Kolmogorov spectrum one has $D_\parallel \propto E^{1/3}$, and in general if the spectrum of the random magnetic field energy satisfies $\mathrm{d}E_r/\mathrm{d}k \propto k^{m-2}$, one has $D_\parallel \propto E^m$.

The diffusion orthogonal to the regular magnetic field direction is typically much slower (unless the turbulence level is very high, in which case parallel and perpendicular motions become similar), and it is due to both pitch angle scattering and to the wandering of the magnetic field lines themselves, which drag with them the diffusing particles in the direction perpendicular to $\mathbf{B}_0$. Its evaluation has then to be done numerically, and recent results [2] show that for fixed levels of turbulence (i.e. for given values of $\sqrt{\langle \mathbf{B}_r^2 \rangle}/B_0$) the associated diffusion coefficient $D_\perp$ has a similar energy dependence as $D_\parallel$ as long as $r_L < L_{max}$.

The third ingredient is the antisymmetric (or Hall) diffusion[3], which is associated to the drift of the CRs moving across the regular magnetic field. What is relevant here is the macroscopic drift associated to the gradient of the CR density, which leads to a current

$$J_A = D_A \frac{\mathbf{B}_0}{B_0} \times \nabla N. \qquad (4)$$

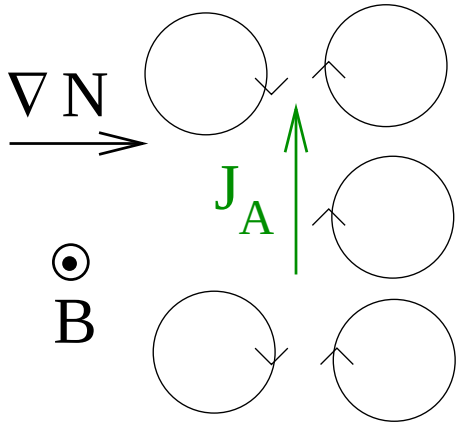

Figure 2. Illustration of the physical origin of the macroscopic drift.

Notice that this macroscopic current is orthogonal to both $\mathbf{B}_0$ and ∇N, and its relation to the microscopic drift associated to gradients and curvature in $\mathbf{B}_0$ is subtle[4]. In particular, the macroscopic drift is also present for a constant $\mathbf{B}_0$, and its origin is illustrated in Fig. 2. The antisymmetric diffusion coefficient is just given by

$$D_A \simeq \frac{r_L c}{3} \propto E. \tag{5}$$

The CR density distribution in the Galaxy is then determined by the equation

$$\nabla \cdot J_D = Q, \text{ with } J_{Di} = -D_{ij}\nabla_j N, \tag{6}$$

where Q describes the distribution of sources and the diffusion tensor is (adopting here the z axis along the direction of $\mathbf{B}_0$)

$$D_{ij} = \begin{pmatrix} D_\perp & D_A & 0 \\ -D_A & D_\perp & 0 \\ 0 & 0 & D_\parallel \end{pmatrix}. \tag{7}$$

To solve equation (6) it is convenient to assume for simplicity that the Galaxy has cylindrical symmetry and that the magnetic field is azimuthal, what is not far from being true, in which case $D_\parallel$ plays no role and one has

$$J_D \simeq -D_\perp \nabla N + D_A \frac{\mathbf{B}_0}{B_0} \times \nabla N, \tag{8}$$

so that the turbulent diffusive component is orthogonal to the isodensity contours while the drifts are parallel to them.

Hence, adopting a realistic configuration of magnetic fields, obtaining from them the diffusion tensor everywhere in the Galaxy (using in particular fits to

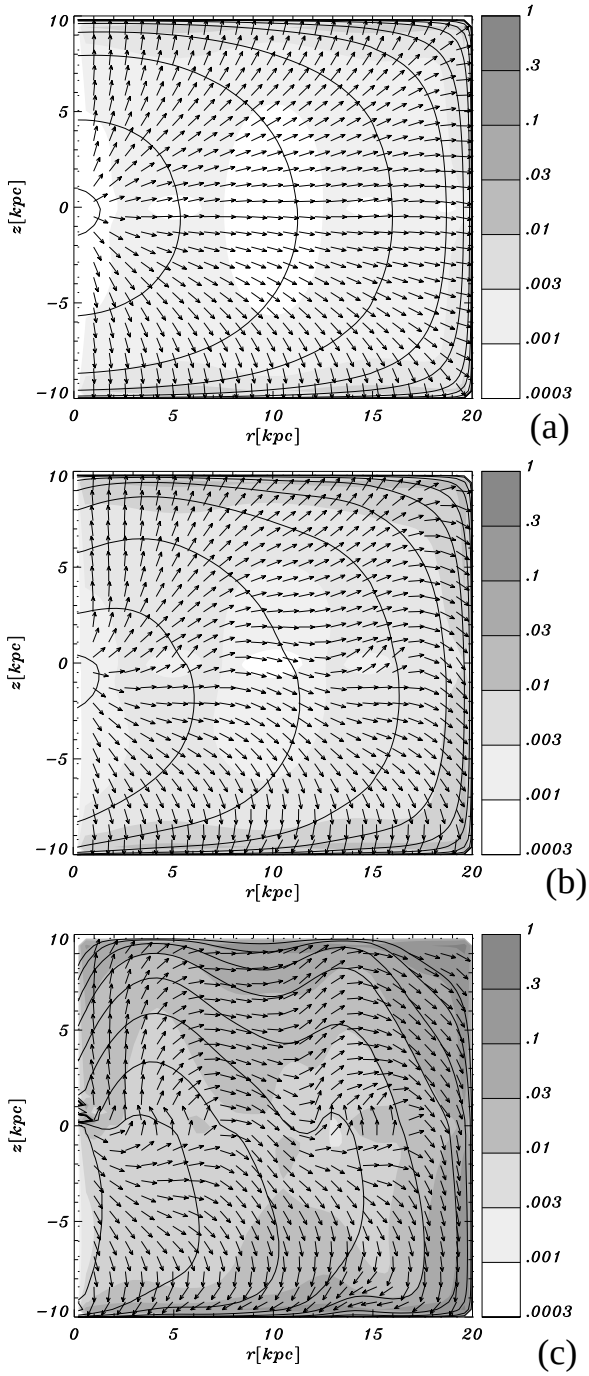

Figure 3. CR isodensity contours for $E/Z = 10^{14}$, 3×10^{15} and 5×10^{17} eV (from top to bottom). The arrows indicate the directions of the diffusion currents while the shading the level of anisotropy.

the numerical results obtained for $D_\perp$ for different turbulence levels[2]), assuming a distribution of CR sources and then numerically solving the diffusion equations, one can obtain[5,6] the CR density distribution in the Galaxy and the resulting diffusion currents. This is exemplified in Fig. 3, which shows the isodensity contours (every two solid contours correspond to a change in density by an order of magnitude) for a source of constant strength in the inner 3 kpc of the galactic plane. The arrows indicate the direction of the diffusion currents, with the component parallel to the contours arising from the drifts. Notice that since the motion of a charged particle in a magnetic field is determined just by its rigidity, the relevant variable is the ratio E/Z. The three panels shown correspond to $E/Z = 10^{14},\ 3\times10^{15}$ and 5×10^{17} eV, and it is clearly seen that for energies below ZE_k the dominant effect arises from the perpendicular diffusion, while for larger energies the drifts are responsible for the dominant escape mechanism. The transition between these two regimes is naturally understood from the different energy dependence of the two diffusion coefficients ($D_\perp \propto E^{1/3}$ while $D_A \propto E$). Actually, both coefficients become comparable, $D_\perp \simeq D_A$, at an energy of the order of ZE_k, and this crossover naturally generates the observed break in the spectrum.

2.2 The knee:

If the source spectrum is taken as a power law, $\mathrm{d}Q/\mathrm{d}E \propto E^{-\alpha_s}$, it is seen from the diffusion equation that the observed spectrum will be affected by the energy dependence of the diffusion coefficients. This just reflects the fact that the CR confinement time in the Galaxy is $\tau_e \propto D^{-1}$. Hence, below the knee, where transverse turbulent diffusion dominates, the observed spectral index will be $\alpha \simeq \alpha_s + 1/3$, while in the drift dominated regime one has instead $\alpha \simeq \alpha_s + 1$. Since this transition takes place at different energies for CRs with different charges, one expects that first the proton component will steepen its spectrum at an energy that will be identified with E_k, and then the heavier components will suffer a similar change in their spectrum but at energies ZE_k. This is illustrated in Fig. 4, which shows the local density of the different CR components obtained[5] in the scenario described in Fig. 3. The CR composition is normalized with existing satellite measurements of lower energies, typically below 10^{14} eV, and the individual spectra of H, He, O and Fe are displayed, together with the total flux.

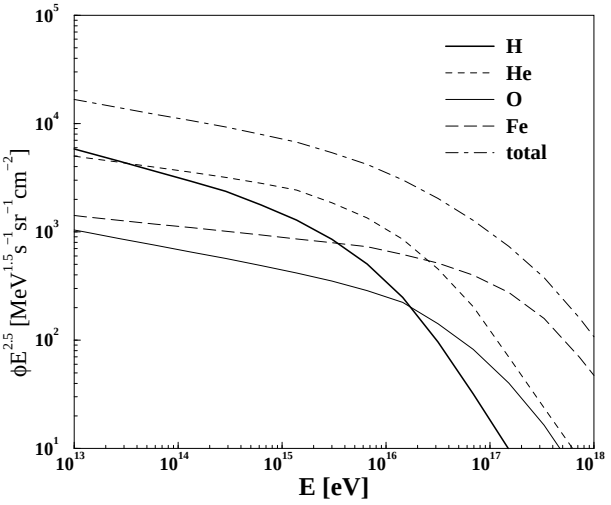

Figure 4. Predicted individual and total spectra in the diffusion/drift scenario.

It is seen that although each individual component changes its spectral index by $\Delta\alpha_i \simeq 2/3$, the total flux has a softer steepening, which is consistent with the measured change of $\Delta\alpha \simeq 0.3$. Here the source spectrum is assumed to have a constant spectral index $\alpha_s \simeq 2.3$ (which is consistent with expectations from first order Fermi acceleration in strong shocks, which typically predict $\alpha_s \simeq 2 \div 2.4$) and the spectral change in the observed spectrum just results from not ignoring the physical effects of the CR drifts. Let us mention that the energy at which the break occurs depends on several things, like the assumed distribution of sources, the location in the Galaxy where the flux is measured, the symmetry of the regular magnetic field, the level of turbulence and the maximum scale of turbulence (scaling in particular as $L_{max}^{-1/2}$). It is very reassuring that for the realistic models adopted it just falls in the energy range where the knee is observed.

2.3 The second knee and the ankle:

Since the heaviest CRs having a significant abundance are the Fe nuclei, once one considers energies above $26 \times E_k \simeq 10^{17}$ eV the light components will be already very suppressed and hence the composi-

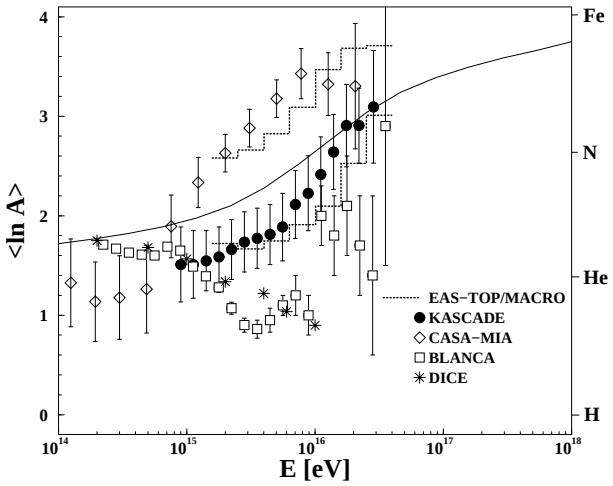

Figure 5. Measured composition and predictions (solid line) of the diffusion/drift scenario.

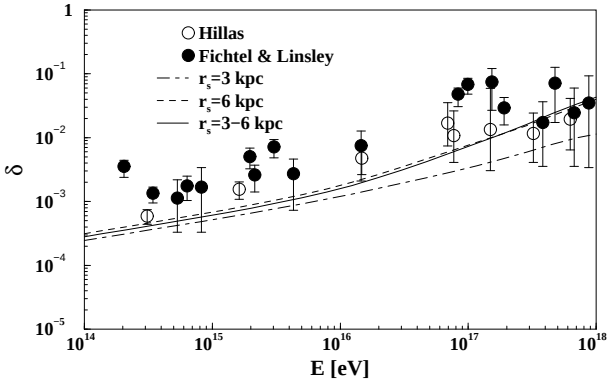

Figure 6. Measured anisotropies (amplitude of the first harmonic in right ascension) and predictions of the diffusion/drift scenario for different assumed source distributions.

tion will be dominated by these heavy nuclei. When drifts then start to affect this component, the total spectrum will gradually steepen to $\alpha \simeq \alpha_s + 1 \simeq 3.3$, which is just the behavior observed at the so-called second-knee. This is illustrated by the different lines depicted in Fig. 1, which show the total spectrum obtained[7] with different magnetic field and source models. In addition, the straight dotted line represents the contribution from extragalactic CRs, with an assumed spectrum $\propto E^{-2.7}$ and normalized to fit observations above the ankle (at energies beyond 5×10^{19} eV, the effects of the GZK suppression by interactions with the CMB photons, not included here, should also be accounted for). It is seen that all the main features of the spectrum below the ankle find a natural explanation in terms of the CR diffusion process.

2.4 Composition and anisotropies:

As regards the composition, the behavior just described implies that the CRs become increasingly heavy beyond the knee. The predictions[5] for the average mass number ($\langle \ln A \rangle$) are displayed in Fig. 5, together with the observational data on this quantity. Although there was a large spread on the measured values, the most recent results from the KASCADE[8] and the MACRO/EAS-TOP[9] Collaborations are in quite good agreement between them and with the theoretical predictions of the diffusion/drift scenario. Moreover, KASCADE has reported a measurement of the spectra of four different mass groups (H, He, C, Fe) and they are remarkably consistent with the predictions depicted in Fig. 4. On the other hand, the MACRO/EAS-TOP experiment has found that the change in the spectral slope of the individual components is $\Delta\alpha_i = 0.7 \pm 0.4$, consistent with the value of 2/3 induced by the drifts.

Regarding the anisotropies, if the knee is actually due to a change in the escape mechanism from the Galaxy (rather than a change in the intrinsic source spectra), one expects to find a correlation between the change in the behavior of the energy spectrum and of the CR anisotropies. This is in fact what seems to be observed, and the predicted[6] anisotropies are in good agreement with the observational results, as is apparent from Fig. 6.

Let us mention that several possible mechanisms have been proposed in the past to explain the knee. For instance, that it could be associated to the heavy CR components being photodisintegrated by interactions with optical or UV photons inside the sources[10]. This scenario would predict for instance that the composition should become lighter above the knee, at odds with the latest observations mentioned previously. It has also been suggested that the knee could be related to a change in the efficiency of CR acceleration in the sources. This is attractive since the traditional acceleration scenario based on supernovae exploding in the ISM is expected to lead to maximal energies of about $E/Z \sim 10^{14} \div 10^{15}$ eV. However, these scenarios (and also the one with photodisintegrations) would have difficulties to account for the CR anisotropies observed, for the origin of

the second knee and, in any case, since drift effects are anyhow present, they will have to be taken into account and would lead to further suppressions beyond those originating in the sources. Other acceleration mechanisms, such as supernovae exploding in the wind of their progenitors or one-shot acceleration in pulsars, may naturally reach larger values of E/Z, so that the assumption that α_s remains constant beyond E_k is quite plausible.

3 Cosmic Ray induced neutrino fluxes

When CRs interact in the upper atmosphere producing particle cascades, a very important product which results are the fluxes of muon and electron neutrinos, which arise mainly from the decays of charged pions and kaons. The study of these atmospheric neutrinos has been of paramount importance in recent years, allowing in particular to establish the existence of neutrino flavor oscillations, and hence of neutrino masses and mixings. One may then say that in this respect CRs have returned to be a source of particle beams of great interest for particle physics.

Also the interactions of galactic CRs with the gas present in the ISM is expected to yield fluxes of high energy neutrinos from directions close to the galactic plane (ISM ν's). Actually, the associated fluxes of high energy photons from π^0 decays have already been observed by EGRET. In addition, several galactic (supernova remnants, microquasars, ...) and extragalactic (active galaxies, gamma ray bursts, ...) objects are also potential sources of very high energy neutrinos, being the target of the ongoing and projected neutrino observatories (Amanda, Baikal, Antares, Auger, Icecube, ...). Since the flux sensitivities achieved are expected to improve by more than two orders of magnitude in the next decade[11], this will open a new window to explore the Universe by means of the high energy neutrinos. These messengers have the great advantage of arriving undeflected and unattenuated from their sources, containing then precious information about their production sites.

CRs with energies beyond E_k will produce atmospheric neutrinos (and ISM νs) with very high energies, typically $E_\nu > 10^{14}$ eV. Atmospheric neutrinos with these energies are particularly interesting because they are expected to arise mainly from the decays of mesons containing charm quarks, since these decay "promptly" after being produced while,

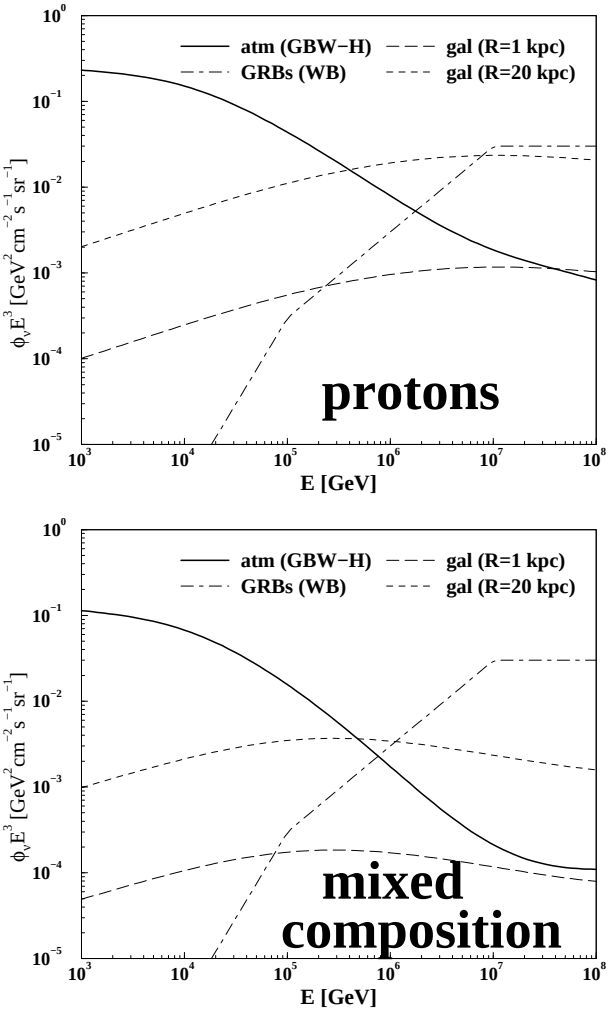

Figure 7. CR induced neutrino fluxes under the assumption that the CR are only protons (top) or have a mixed composition (bottom), as results in rigidity dependent explanations of the knee. The solid line is the flux of atmospheric neutrinos, the dashed lines are the ISM νs from the direction of the galactic center (upper) or perpendicular to the galactic plane (lower line). Also indicated is the ν flux from GRBs predicted by Waxman and Bahcall.

due to the relativistic time dilation, the pions and kaons have decay lengths much larger than 10 km at these energies, and are hence stopped by the atmosphere before they can decay, so that the neutrinos they produce have much lower energies.

To evaluate the fluxes of prompt neutrinos is quite delicate, since it requires[12] to take into account next to leading order processes in the charm production cross section, which also turns out to depend on the behavior of the parton distribution functions (PDF) at very low values ($x < 10^{-4}$) of the fraction of momentum carried by the partons, and these values are below those that can be measured with present accelerators. It has been actually suggested that the observations of very high energy atmospheric neutrinos could be used to study the PDFs in the range $10^{-9} < x < 10^{-4}$. Moreover, it is important to know these fluxes in detail because they constitute the main background for the search of some astrophysical neutrino sources.

To predict these fluxes it actually turns out that one needs a detailed knowledge of the CR composition beyond the knee, since a heavy CR nucleus of mass A behaves just as a collection of A nucleons of energy E/A. Hence, if the CRs are heavy they will produce fluxes of neutrinos of much lower energies, what combined with the steepness of the CR spectrum implies a much reduced neutrino flux. This is illustrated in Fig. 7, which shows the neutrino fluxes predicted under the (standard) assumption that CRs consist mainly of protons as well as the predictions adopting the composition which results in models where the knee is a rigidity dependent effect (such as the diffusion/drift scenario just discussed), and for which the composition becomes heavier above the knee[13]. Clearly this implies that the CR induced neutrino fluxes will be harder to detect, but also that the background for the search of other astrophysical neutrino sources (such as the GRB prediction also shown in the figure) will be reduced.

4 Magnetic lensing

CRs have a diffusive propagation in the Galaxy as long as their Larmor radius stays smaller than the maximum scale of the turbulence, i.e. for E/Z below a few times 10^{17} eV (see Eq. (1)). It is only at higher energies that the trajectories gradually straighten up and that it may become possible to attempt to do

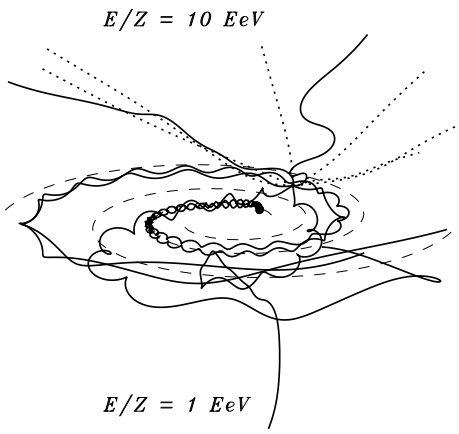

Figure 8. CR trajectories reaching the Earth for energies $E/Z = 10^{18}$ eV (1 EeV, solid lines) and $E/Z = 10^{19}$ eV (10 EeV, dotted lines). The dashed lines indicate the location of the galactic spiral arms.

"CR astronomy", i.e. to try to identify the images of individual CR sources. This is illustrated in Fig. 8, which shows[14] several trajectories of CRs reaching the Earth. At energies $E/Z = 10^{18}$ eV CRs are strongly deflected and there is no way in which the direction of arrival to the Earth can give information about the original source direction, while for $E/Z = 10^{19}$ eV the deflections start to become manageable.

The transition between the diffusive behavior to the regime of small deflections is actually very rich in new phenomena and several qualitatively different regimes appear.

4.1 The regime of small deflections:

Starting from the high energy end, we can expect that CRs arriving from distant sources will suffer only small deflections, so that an image with a slight (rigidity dependent) offset with respect to the original source position should be observed. If the intervening magnetic field and the CR charge were known, this effect could in principle be corrected in order to infer the source coordinates[15,16,17]. To have an idea about the deflections involved, one can keep in mind that the deflection in the direction of the trajectory of a CR traversing a distance L across a constant magnetic field B is

$$\delta \simeq 3.2^\circ \frac{10^{20}\ \mathrm{eV}}{E/Z} \frac{L}{3\ \mathrm{kpc}} \frac{B}{2\ \mu\mathrm{G}}. \qquad (9)$$

Hence, the regular galactic magnetic field can produce sizeable deflections even for CRs with the highest energies observed, specially if their composition is heavy. It has to be said however that almost nothing is known about the CR composition above the ankle, and this is one of the issues that the future large statistics observatory AUGER is expected to clarify.

Notice that although the random magnetic field has an rms strength similar to the regular magnetic field strength, its effects on the overall CR deflections is smaller, due to its short coherence length[a] L_c, which results in a deflection growing only as $\sqrt{L/L_c}$, where L/L_c is just the number of magnetic "domains" traversed. Indeed, the rms deflection it induces is

$$\delta_{rms} = 0.6^\circ \frac{10^{20}\ \mathrm{eV}}{E/Z} \frac{B_{rms}}{4\ \mu\mathrm{G}} \sqrt{\frac{L}{3\ \mathrm{kpc}}} \sqrt{\frac{L_c}{50\ \mathrm{pc}}}. \quad (10)$$

The random component has however important effects on the lensing of CRs. Let us also mention that extragalactic magnetic fields can further affect the CR trajectories[18,19,20]. Their effects could be significant if they have sizeable strength and large coherence lengths (i.e. if $B \times \sqrt{L_c} > 10^{-9}$ G$\sqrt{\mathrm{Mpc}}$).

4.2 The lensing regime:

When the deflections produced by the magnetic fields are such that the CRs can arrive to the observer through paths which deviate from the straight one by more than the scale of coherence of the magnetic field (e.g. a few kpc for the regular field or the scale L_c for the random component), it becomes possible for the CRs to reach the observer through different, uncorrelated, paths. This just means that several different images of the same source will appear. This phenomenon is quite similar to the well known gravitational lensing phenomena, but here it is the magnetic deflection that replaces the gravitational one. Contrary to this last one, the magnetic deflections are energy dependent, so that the multiple images would look differently at different energies. Anyhow, many magnetic lensing phenomena look as a function of energy very similar to some gravitational lensing phenomena as a function of time when the relative motion of the lens is relevant, such as in the microlensing events.

[a]For a Kolmogorov spectrum, one has $L_c \simeq L_{max}/5$.

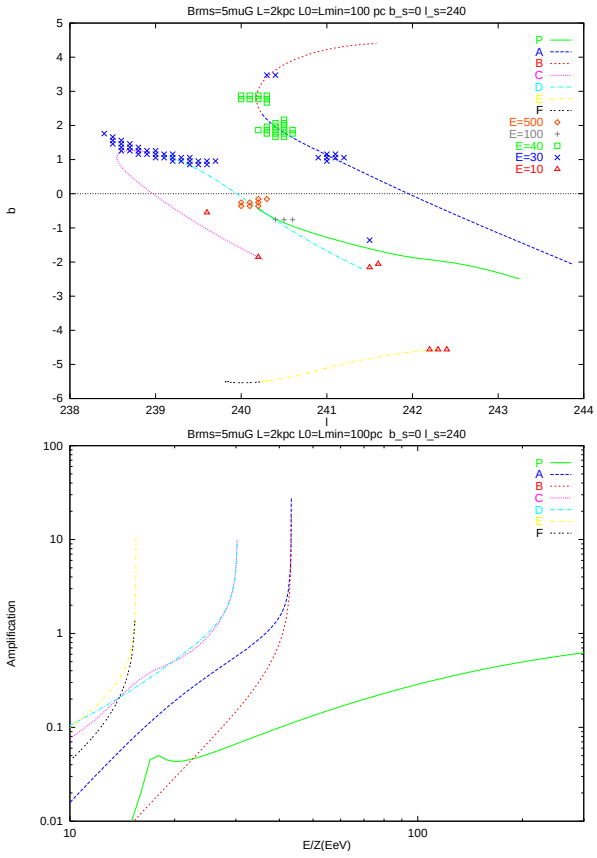

Figure 9. Images (top panel) of a CR source located near $(b, \ell) \simeq (0^\circ, 240^\circ)$. The different symbols correspond to the images obtained through a ray-shooting simulation (assuming an extended source) at energies $E/Z = 500$, 100, 40, 30 and 10×10^{18} eV. New secondary images appear in pairs below some critical energies, and for decreasing energies get displaced along the lines indicated. The bottom panel shows the magnification of the fluxes of the different images.

Besides producing multiple images, the magnetic field can also lead[14,21] to focusing effects which magnify or demagnify the original source fluxes. In particular, when new images appear at a certain energy E_0, they always appear in pairs (which moreover have opposite parities, i.e. one of the images will be inverted, something which in practice is of course unobservable however), and they are magnified by a factor $A \propto (E_0 - E)^{-1/2}$, which diverges[b] for $E \to E_0$. This can lead to huge enhancements in the CR fluxes in narrow ranges of energies.

The multiple image formation is illustrated[22] in Fig. 9, which shows how a particular source will look

[b]The average magnification in a finite energy bin stays of course bounded.

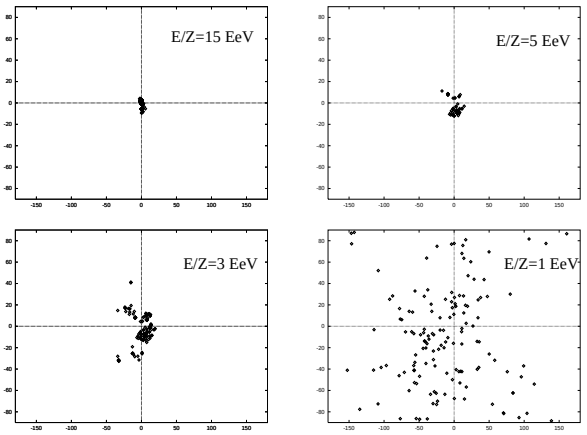

Figure 10. Images of a CR source in the scintillation regime.

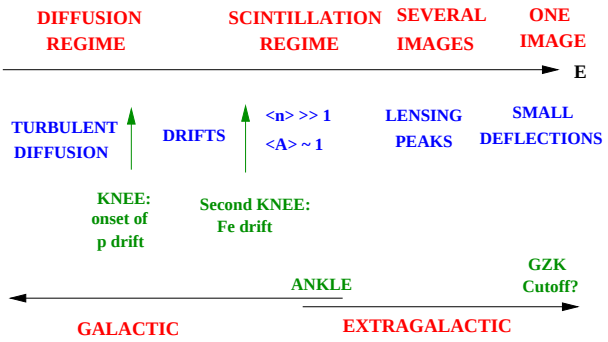

Figure 11. Sketch of the different CR propagation regimes.

like at different energies, and how for decreasing energies new images are produced and continuously displaced. The lensing effects for this same source are illustrated in the second panel, which shows the amplifications of the different images, clearly displaying the presence of lensing peaks when new images appear. These peaks can lead to interesting observational effects, since they will lead to an enhanced number of events in a narrow angular window, corresponding to the direction where the new pair of images appear in the sky, which will also be clustered in energy (or, actually, in rigidity). It is remarkable that this clustering in rigidity seems to be already present[22] in the clusters of pairs and triplets of events with small angular separations observed[23] at the highest energies ($E > 4 \times 10^{19}$ eV). The increase in statistics that will be achieved with Auger will allow these predictions to be tested with higher significance.

4.3 The scintillation regime:

For typical galactic magnetic field models, multiple images of extragalactic CR sources appear at energies $E/Z \sim$ few $\times 10^{19}$ eV. As smaller energies are considered, one can show[22] that the number of secondary images grows exponentially, increasing to about 10^2 in a decade of energy and this trend continues for lower energies. The lensing peaks associated to the new images become increasingly narrow, and the result is that what is observed is just a blurred image, consisting of a very large number of secondary images, with an angular extent determined by δ_{rms} and with an average magnification which approaches unity. This behavior is illustrated in Fig. 10, which shows the results of a ray-shooting simulation displaying the way a given CR source will look like at different energies in the regime in which a large number of images are present.

This "scintillation" regime is reminiscent to the twinkling of stars caused by the refractive effects of the atmospheric turbulence, although in the present case it is the galactic magnetic turbulence the one responsible for the effects observed. This regime is different from the diffusion one, since the deflections δ_{rms} need not be large. Hence, only some small random deflections in the direction of the trajectories are being produced, but in order that the spatial diffusion regime sets in one has to still go down in energy until $r_L < L_{max}$, so that the resonant scattering leading to pitch angle scattering can take place.

A brief summary of the different propagation regimes discussed is shown in Fig. 11.

It is interesting that we are at a time when many of these ideas will be tested with more precise measurements of the CRs both in the region of the knee (with e.g. KASCADE-GRANDE) and at the highest energies (with AUGER), and this will certainly help to unveil some of the many mysteries that CR still present to us.

Acknowledgments

This work is based on several collaborations done with J. Candia, L. Epele, D. Harari and S. Mollerach It is partially supported by the Fundación Antorchas and the John Simon Guggenheim Foundation.

References

1. M Nagano and A Watson, Rev. Mod. Phys. **72** (2000) 689.
2. F Casse, M Lemoine and G Pelletier, Phys. Rev. D **65** (2002) 023002.
3. V S Ptuskin et al., Astron. Astrophys. **268** (1993) 726.
4. R A Burger, H Moraal and G M Webb, Ap& SS **116** (1985) 107.
5. J Candia, E Roulet and L Epele, JHEP 0212 (2002) 033.
6. J Candia, S Mollerach and E Roulet, Journal of Cosmology and Astropart. Phys., JCAP0305 (2003) 003.
7. J Candia, S Mollerach and E Roulet, JHEP 0212 (2002) 032.
8. A Haungs, J. Phys. G **29** (2003) 809.
9. M Aglietta et al. (EAS-TOP/MACRO Collaborations), `astro-ph/0305325`.
10. A M Hillas, 16 ICRC Kyoto, vol. **8** (1979) 7; S Karakula and W Tkaczyk, Astropart. Phys. **1** (1993) 229; J Candia, L Epele and E Roulet, Astropart. Phys. **17** (2002) 23.
11. C Spiering, J. Phys. G **29** (2003) 843.
12. A D Martin, M G Ryskin and A M Staśto, `hep-ph/0302140`; L Pasquali, M H Reno and I Sarcevic, Phys. Rev. D **59** 034020.
13. J Candia and E Roulet, Journal of Cosmology and Astropart. Phys., JCAP0309 (2003) 005.
14. D Harari, S Mollerach and E Roulet, JHEP **08** (1999) 022.
15. T Stanev, Astrophys. J **479** (1997) 290.
16. G Medina Tanco, E De Gouveia dal Pino and J Horvath, Astrophys. J. **492** (1998) 200.
17. D Harari, S Mollerach and E Roulet, JHEP **07** (2002) 006.
18. G Sigl, M Lemoine and P Biermann, Astropart. Phys. **10** (1999) 141.
19. G Medina Tanco, Astrophys. J. **505** (1998) L79.
20. T Stanev, D Seckel and R Engel, `astro-ph/0108338`.
21. D Harari, S Mollerach and E Roulet, JHEP **02** (2000) 035.
22. D Harari, S Mollerach, E Roulet and F Sánchez, JHEP **03** (2002) 045.
23. Y Uchihori et al., Astropart. Phys. **13** (2000) 151.